ejpmr, 2016,3(12), 1-10

SJIF Impact Factor 3.628

EUROPEAN JOURNAL OF PHARMACEUTICAL AND MEDICAL RESEARCH

www.ejpmr.com

Research Article

ISSN 2394-3211

EJPMR

ALLOXAN-DIABETES CAUSES OXIDATIVE IMBALANCE AND MORPHOLOGICAL, MORPHOMETRIC AND ULTRASTRUCTURAL CHANGES IN RAT LUNGS

[1]Olivia A. Xavier Suarez MD, PhD., [1]Amanda Natália Lucchesi BS, PhD., [1]Antônio José M. Catâneo MD, PhD., [1]*César Tadeu Spadella MD, PhD.

[1]Department of Surgery and Orthopedics, Faculty of Medicine of Botucatu, Sao Paulo State University - Unesp, Botucatu, Sao Paulo, Brazil.

Corresponding Author: Dr. César Tadeu Spadella

Department of Surgery and Orthopedics, Faculty of Medicine of Botucatu, Sao Paulo State University - Unesp, Botucatu, Sao Paulo, Brazil.

Article Received on 23/09/2016 **Article Revised on 13/10/2016** **Article Accepted on 02/11/2016**

ABSTRACT

Purpose: This study evaluated the long-term effects of alloxan-induced diabetes in rat lungs. **Method:** Sixty non-diabetic control (NC) and 60 untreated diabetic (UD) rats were divided into 3 subgroups and sacrificed after 6, 14, or 26 weeks. **Results:** UD rats showed clinical and laboratory signs of severe diabetes throughout the study. Fresh and fixed lung weight, fixed lung volume, and lung compliance were significantly reduced in UD rats, whereas fresh lung weight relative to body weight was higher after 14 and 26 weeks. LPO free radicals were significantly higher in the pulmonary tissue of UD rats, whereas SOD, CAT, and GSH-Px antioxidant enzyme activities were lower after 14 and 26 weeks. UD rats showed lung morphological changes characterized by diminution of alveolar spaces with alveolar septa thickening and varying degrees of congestion, insudation, and interstitial mononuclear inflammatory infiltrate. Morphometric analysis revealed that the total number of alveoli and alveolar and endothelial basal laminae thickness were significantly higher in UD than NC rats, whereas alveolar perimeter and alveolar surface area were decreased. Ultrastructural changes were observed in all structures of UD alveolar septa and included alveolar and capillary lumen narrowing, type I cell degeneration, expansion of interstitial extracellular matrix by edema and abundant pynocytotic vesicles, and diminution of type II cell microvilli, which had a high amount of mature lamellar corpuscles with a delay in their surfactant output out of the cytoplasm. **Conclusions:** Alloxan-diabetes causes morphological, morphometric and ultrastructural changes in rat lungs. These changes may be correlated to oxidative imbalance caused by persistent hyperglycemia.

KEYWORDS: Diabetes Mellitus. Alloxan Diabetes. Diabetic Chronic Lesions. Pulmonary Changes. Morphology. Ultrastructure.

INTRODUCTION

Diabetes mellitus (DM) is a chronic degenerative metabolic disease that is currently considered one of the greatest problems of global public health. It affects the survival and quality of life for millions of people around the world due to its acute and chronic complications on the cardiovascular system, kidneys, retina, and nerves.[1.2.3]

However, several studies suggest that the lungs may also be affected by DM because various respiratory function abnormalities have been observed in diabetic subjects involving lung volume, pulmonary diffusing capacity, control of ventilation, bronchomotor tone, and neuroadrenergic bronchial innervation.[4.5]

Nevertheless, unlike cardiovascular disease, nephropathy, retinopathy, and neuropathy, diabetic pneumopathy has not been fully explored in the literature, mainly involving studies on the course of morphological, morphometric and ultrastructural changes of the lungs under a chronic hyperglycemia regime without any treatment over a long period of follow-up.[6.7.8]

Moreover, although hyperglycemia has been recognized as the causal link between diabetes and chronic complications, the causative mechanisms of diabetic lesions are still widely discussed.[9.10] A previous study performed in our laboratory showed that oxidative stress from increased generation of reactive oxygen species (ROS) can play an important role in the genesis and progression of kidney injury in alloxan-induced diabetic rats. [11] Thus, we believe that oxidative stress may also be one of the mechanisms responsible for the development and progression of lung injury and other chronic diabetic lesions.

Therefore, the aim of the present study was to investigate the long-term effects of alloxan-induced DM on the lung tissue of rats maintained with high levels of blood glucose compared to age-matched normal control rats

with an equal follow-up period. We also hope to establish the relationship between pulmonary oxidative balance and the lesions found in lungs.

MATERIAL AND METHODS

Animals and groups

One-hundred and twenty male Lewis rats, approximately 12 weeks old, were randomly assigned to two experimental groups: UD – 60 alloxan-untreated diabetic, and NC – 60 non-diabetic control rats. Each group was further divided into 3 subgroups of 20 rats each, which were sacrificed after 6, 14 and 26 weeks of follow-up. At the time of sacrifice, the animals from the two groups were 18, 26 and 38 weeks old, respectively.

The use of laboratory animals followed the ethical code for animal experimentation of the International Council for Laboratory Animal Science (ICLAS) and was approved by the Animal Experimentation Ethics Committee of our institution.

Diabetes induction and techniques

Diabetes was induced by alloxan (Sigma Co., Cream Ridge, NJ, USA) intravenously using one of the tail veins in a single dose of 42 mg/kg body weight. Only diabetic rats showing a severe diabetic state with fasting glucose >250 mg/dL were included in the experiment. In a similar procedure, NC rats received 1 ml of saline. Any animals that died after diabetes induction or during follow-up were replaced by standbys in their respective subgroups to avoid compromising the final number of rats in the sample. Diabetic animals affected by pneumonia, pyoderma and/or pediculosis were treated with antibiotics or topical antiparasitic applications, respectively. After diabetes induction, the rats from the UD group were left without any control of hyperglycemia until the end of the experiment, while having age-matched non-diabetic rats with equal follow-up period served as controls.

Animals from both experimental groups were sacrificed under general anesthesia using ketamine cloridrate at a dose of 100 mg/kg body weight, associated with xylazine cloridrate at a dose of 25 mg/kg body weight, administered intramuscularly (Rhobifarma Ind. Farmacêutica, Hortolândia, SP, Brasil). Blood was collected during follow-up by cutting a section from the distal end of the tail and at the time of sacrifice via cardiac puncture, with the chest open. Euthanasia was performed by exsanguination, followed by infradiaphragmatic sectioning of the vena cava.

Clinical and laboratory analysis

At 2 weeks after initiation of the experiment or diabetes induction (initial parameters) and after 6, 14 and 26 weeks of follow-up, rats from the two experimental groups were housed in metabolic cages to measure their body weight, 24-hour water intake, 12-hour food intake, 24-hour urine volume, blood and urinary glucose, glycosylated hemoglobin (HbA1c) and plasma insulin. Blood and urinary glucose were measured via a standard enzymatic method (Johnson & Johnson Inc., New Brunswick, NJ – USA), HbA1c via agarose gel electrophoresis (Sebia Inc., Norcross, GA, USA), and plasma insulin via radioimmunoassay using a Coat-A-Count kit (Diagnostic Products Co., Los Angeles, CA, USA).

Macroscopy and lung tissue analysis

After anesthesia, a midsternotomy was performed, and the lungs and heart were removed "en bloc" and then further separated. The lungs from 10 rats in each subgroup were excised and immediately weighed to obtain fresh weights (g). The mass of both fresh lungs relative to the body weight (g/100 g) was also calculated in each study period. Then, a 20 G endotracheal tube was tied in place to obtain lung compliance. Thus, the lungs were inflated with 10% phosphate buffered formaldehyde. Fixed lung volumes (ml) were calculated by the quantity of formalin used for lung inflation and lung compliance by the ratio between the volume of formalin infused and the perfusion pressure used, which was maintained at 25 cm H_2O. Lungs were maintained inflated for fixing with 10% formalin for 72 h and further used for scanning light microscopy. Lung tissue from 10 other rats in each subgroup was used to evaluate pulmonary oxidative stress and ultrastructural analysis for transmission electron microscopy.

Biochemical markers of oxidative stress

Fresh pulmonary tissue of each sacrificed animal from two experimental groups was analyzed for oxidative stress markers, namely lipid hydroperoxide (LPO) concentration and superoxide dismutase (SOD), catalase (CAT), and glutathione peroxidase (GSH-Px) enzyme activities using specific reagents (Cayman Chemical Co., Ann Arbor, MI, USA).

Morphological and Morphometric Analysis

After fixing, 5 lungs from each subgroup sacrificed at 6, 14 and 26 weeks were randomly cut sagittally, and fragments from the midsagittal slice were obtained. They were embedded in paraffin, cut into 5-µm-thick slices and stained with hematoxylin and eosin (HE). The presence of fatty deposits in the pulmonary artery endothelium and their trunks was examined using the oil red staining. For morphological and morphometric analysis, images of 20 histological sections of each lung were captured at final magnifications ranging from 100 to 400x and digitized, using an optical microscope connected to a computerized digital image system; thus, a total of 100 histological sections were analyzed per subgroup of rats. In the morphological analysis, the pulmonary cytoarchitecture, alveolar wall thickening, and the presence of transudate, edema, congestion, hemorrhage, and inflammatory infiltrate, intra-alveolar and/or interstitial, were analyzed. Morphometric studies were performed using a KS-300 image analyzer and software. The total number of alveoli/μm^2, alveolar perimeter (µm), and alveolar surface area (μm^2) were

measured. For the morphometric analysis, cross-sections of 50 random pulmonary alveoli were measured in each rat lung, and in total, 250 measurements were performed for each analyzed parameter. Only alveoli with a well-defined and complete structure were selected, and any alveolus cut tangentially was excluded from the analysis. All analyses were performed by the same investigator who was unaware of the experimental group to which the material belonged.

Ultrastructural analysis

Lungs from 5 random rats in each subgroup were removed after 6, 14 and 26 weeks of follow-up. They were sagittally cut into 3-mm-thick slices and pre-fixed in 2.5% glutaraldehyde for 30 minutes. After pre-fixing, lungs were again cut into 1-mm-thick cylindrical fragments, post-fixed in osmic acid, dehydrated, and embedded in epoxy resin (Araldite). Five tissue blocks were prepared from each lung, and ultrathin sections were examined by transmission electron microscopy at final magnifications between 6,500 and 42,000x. Ten electron micrographs were taken from each lung tissue block, giving a total of 50 micrographs per evaluation time. Wherever possible, electron micrographs were taken of structures with linear images and without angles or artifacts. Tangentially sectioned capillaries were excluded from analysis. In this investigation, we analyzed the structure of the alveolar septa and capillary lumen, the type 1 and type 2 pneumocytes, and the surfactant density. Alveolar epithelial (AE) and endothelial capillary (EC) basal laminae (BL) thickening at three distinct points in the membranes was also measured. Digital image morphometry with a Leica Quin Lite 2.5 was used to measure BL thickening. Values were expressed as means ± SD of the three measurements taken (µm).

Statistical analysis: Clinical and laboratory data, absolute and relative fresh lung weights, fixed lung weights, fixed lung volumes, lung compliance, and morphometric data were analyzed via one-way analysis of variance (completely randomized design), complemented with multiple-comparison tests according to Tukey-Kramer (homogeneous variables) or Mann-Whitney and Kruskal-Wallis (heterogeneous variables). All statistical analyses were based on a significance level of 5% (P<0.05).

RESULTS

Clinical and laboratory findings

NC rats had clinical and laboratory parameters consistent with those observed in animals of the same strain throughout the study period. In contrast, UD rats without any hyperglycemic control evolved with low body weight gain and significant increases (P <0.01) in water intake, food intake and urine output compared with NC animals. Blood and urine glucose levels and glycosylated hemoglobin were also consistently elevated in diabetic rats, and plasma insulin levels were significantly lower than that in the NC rats (P <0.001). The clinical and laboratory data are shown in Fig. 1 and Fig. 2.

UD rats showed a significant reduction in fat mass and muscle in the entire body compared to NC rats. This weakness of body mass was more evident in animals sacrificed at 26 weeks of follow-up. UD rats also showed frequent episodes of skin infections (pyoderma) and were also more prone to pneumonia and lice infestations.

There were no deaths in the NC group. Approximately 32% from the initial lot of animals that received alloxan died in the first two weeks after diabetes induction due to metabolic disorders and drug toxic action. Another 15% were not diabetic or evolved with mild or moderate diabetes (<250 mg/dL) and were excluded from the experiment. Of the 60 UD animals placed in follow-up, approximately 13% died in late follow-up (up to 26 weeks), primarily due to ketoacidosis (1 rat) and pulmonary infection (7 rats).

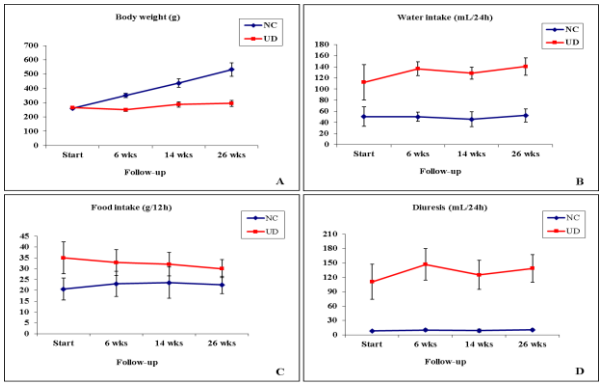

Figure 1: Mean ± SD of body weight (A), water intake (B), food intake (C) and diuresis (D) observed in rats from the two experimental groups.

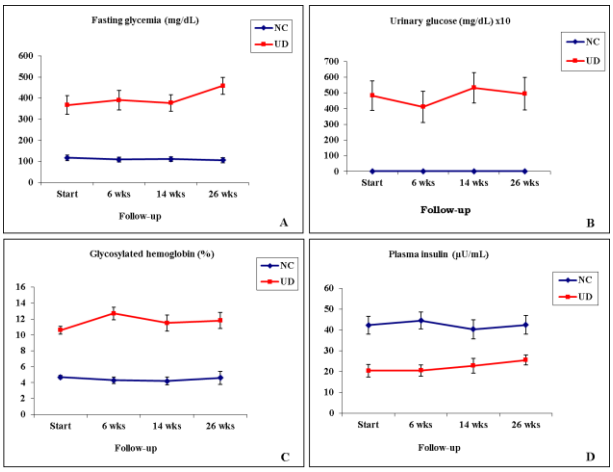

Figure 2: Mean ± SD of fasting glycemia (A), urinary glucose (B), glycosylated hemoglobin (C), and plasma insulin (D) observed in rats from the two experimental groups.

Pulmonary oxidative stress markers

The LPO concentration in pulmonary tissue of the UD rats was significantly higher than that in the NC rats (P < .01) at 6, 14, and 26 weeks of follow-up. There were

significant (P < .01) reductions in SOD, CAT and GSH-Px enzyme activity values in UD pulmonary tissue at 14 and 26 weeks after diabetes induction compared with NC. Pulmonary oxidative stress was also strongly related to diabetes duration and was more intense after the 14th week of diabetes. Table 1 shows these data.

Table 1: Lipid hydroperoxide concentration (LPO) and superoxide dismutase (SOD), catalase (CAT), and glutathione peroxidase (GSH-PX) pulmonary tissue enzyme activities in the two experimental groups.

		Follow-up		
Parameters	**Groups**	**6wks**	**14wks**	**26wks**
LPO (nmol/g)	NC	40.67 ± 0.52	41.21 ± 0.49	46.58 ± 0.78
	UD	71.30 ± 0.53*	77.80 ± 0,55*	98.25 ± 0.86*
SOD (U/g)	NC	81.37 ± 0.64	79.48 ± 1.05	70.47 ± 0.93
	UD	78.40 ± 1.28^{ns}	53.23 ± 0.59*	47.53 ± 1.20*
CAT (µmol/g)	NC	67.84 ± 0.74	64.75 ± 1.46	66.48 ± 0.98
	UD	66.50 ± 1.15^{ns}	50.76 ± 1.02*	41.58 ± 1.23*
GSH-Px (µmol/min/g)	NC	11.63 ± 0.63	10.30 ± 0.50	6.68 ± 0.37
	UD	10.86 ± 0.76^{ns}	5.51 ± 0.32*	3.27 ± 0.56*

*LPO: ***** NC < UD: P < .01 at 6, 14, and 26 wks; SOD/CAT/GSH-Px: ^{ns} NC = UD: P > .10 at 6 wks; SOD/CAT/GSH-Px: ***** NC > UD: P < .01 at 14 and 26 wks.*

Macroscopy analysis

Absolute and relative fresh lung weights

Fresh lung weights were significantly reduced in UD rats compared with NC rats (P<.001) throughout the study. In contrast, considering the ratio of fresh lung weights relative to body weights, the values were significantly higher than those in NC rats at 14 and 26 weeks of follow-up (P<.01); (Table 2).

Fixed lung weights, fixed lung volumes and lung compliance

Fixed lung weights, fixed lung volumes, and lung compliance were also significantly reduced in UD rats compared with NC rats (P<.0001) throughout the study (Table 3).

Table 2: Mean ± SD of fresh lung weights (g), and ratio between fresh lung weights and body weights (flw/bw) in rats from the two experimental groups

		Parameters		
Groups	**Follow-up (weeks)**	**fresh lung weights (g)**	**body weights (g)**	**Ratio: flw/bw**
NC	6	2.20 ± 0.21	350.5 ± 15.6	0.0062
	14	2.37 ± 0.36	436.4 ± 30.0	0.0054
	26	2.16 ± 0.26	532.0 ± 47.3	0.0040
UD	6	1.52 ± 0.11**	250.2 ± 10.5**	0.0060^{ns}
	14	1.88 ± 0.87**	288.2 ± 18.6**	0.0065*
	26	1.83 ± 0.78**	295.4 ± 20.8**	0.0061*

*^{ns} NC = UD:P>.10 at 6 wks; ***** NC<UD:P<.05 at 14 and 26 wks; ****** NC>UD:P<.01 at 6, 14 and 26 wks*

Table 3: Mean ± SD of fixed lung weight (g), fixed lung volumes (mL), and lung compliance in rats from the two experimental groups.

		Parameters		
Groups	**Follow-up (weeks)**	**fixed lung weights (g)**	**Infused volume (mL)**	**lung compliance (mL/cm H_{2O})**
NC	6	10.92 ± 0.64	12.15 ± 0.11	0.6075 ± 0.008
	14	13.19 ± 0.83	12.58 ± 0.07	0.6290 ± 0.020
	26	12.86 ± 0.92	12.66 ± 0.76	0.6330 ± 0.013
UD	6	7.36 ± 0.92*	9.07 ± 0.08*	0.4538 ± 0.004*
	14	6.99 ± 1.07*	9.00 ± 0.16*	0.4502 ± 0.008*
	26	7.08 ± 0.80*	8.96 ± 0.94*	0.4480 ± 0.008*

**NC > UD: P< .0001 at 6, 14, and 26 wks.*

Morphologic findings

UD rats showed histopathological changes in the lungs, which included varying degrees of congestion, insudation, intra-alveolar plasmorrhagy and interstitial mononuclear inflammatory infiltrate, affecting almost the entire lung parenchyma. Decreased alveolar spaces with alveolar septa thickening characterized by increased interstitial extracellular matrix were mainly observed in UD rat lungs sacrificed later at 14 and 26 weeks of follow-up. Despite the severity of morphological lesions in UD rat lungs, lesions or fatty deposits were not observed in the endothelium of the pulmonary arteries and their trunks, even in animals sacrificed later. All morphological abnormalities observed in NC rats were

consistent with those expected for their age for the same period of follow-up. Fig. 3 illustrates the morphological findings in rats from the two experimental groups.

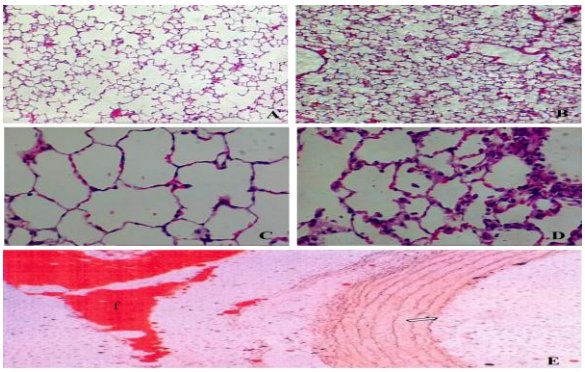

Figure 3: Lung alveoli of non-diabetic control (NC) and untreated diabetic (UD) rats sacrificed at 26 weeks of follow-up. Note in A: alveolar structure of NC rats, showing the alveolar space areas with normal dimensions and alveoli quantity preserved in number (HE 10x); B: alveolar structure of UD rats, showing decreased alveolar space areas and increased number of alveoli (HE 10x), which indirectly shows the lower alveolar distension; C: morphological structure of the alveolar septa of NC rats, showing thin walls with no inflammatory changes (HE 40x); D: morphological structure of the alveolar septa of UD rats showing thickening and intense interstitial mononuclear inflammatory infiltrate, with fibroblasts and collagen filling all of the alveolar interstitium (HE 40x); E: Histologic section of the pulmonary artery wall showing the intimal layer of the vascular endothelium with no lesions and fatty deposits (arrow). Note the presence of normal fatty tissue (f) in the vascular interstitium (oil red - 40x).

Morphometric Analysis

The total number of alveoli in UD rat lungs was higher than that observed in NC, whereas alveolar perimeter and surface area were significantly reduced throughout the study (P<.01). Table 4 shows the morphometric findings in rat lungs from the two experimental groups.

Table 4: Mean ± SD of the total number of alveoli/μm^2, alveolar perimeter (μm) and alveolar surface area (μm^2) in lungs of rats from the two experimental groups.

Parameters				
Groups	**Follow-up (weeks)**	**Total number of alveoli/μm^2**	**Alveolar perimeter (μm)**	**Alveolar surface area (μm^2)**
NC	6	94.82 ± 17.37	1,207.39 ± 533.60	22,187.34 ± 3,238.00
	14	102.71 ± 17.12	1,268.80 ± 326.04	22,746.04 ± 2,202.70
	26	112.68 ± 18.36	1,116.30 ± 285.02	21,814.02 ± 1,692.50
UD	6	129.09 ± 23.83*	182.62 ± 62.43*	14,611,11 ± 1,255.40*
	14	133.48 ± 18.42*	242.10 ± 76.40*	14,027.03 ± 1,932.60*
	26	140.56 ± 19.75*	186.20 ± 66.40*	13,145.30 ± 1,386.80*

**NC< UD: P< .001 at 6, 14, and 26 wks for total number of alveoli; *NC>UD: P<.001 at 6, 14, and 26 wks for alveolar perimeter and alveolar surface area.*

Ultrastructural analysis

Changes compromising all structures of the interalveolar septa were observed in UD rat lungs as early as 6 weeks of diabetes. These changes were markedly severe in rats sacrificed at 26 weeks of diabetes compared with NC rat lungs where ultrastructural changes have not been seen or had little intensity. Among the various types of lung injuries observed in UD rats, the main alterations included the thickening of the alveolar epithelial (AE) and endothelial capillary (EC) basal laminae, the narrowing of the alveolar and capillary lumen, type I alveolar cell degeneration, the expansion of the alveolar interstitium, and type II alveolar cell disorganization characterized by diminution of the amount of microvilli and a delay in the surfactant output out of the cell cytoplasm. Despite this alteration, the number of lamellar bodies in type II alveolar cells was apparently normal. Fig. 4 illustrates the ultrastructural findings of rat lungs in the two experimental groups.

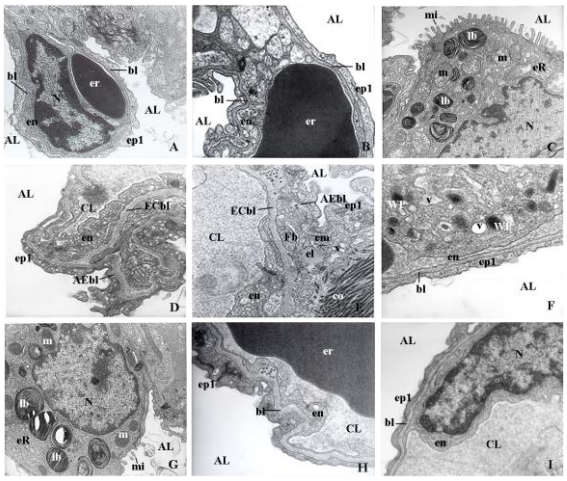

Figure 4: Electron micrographs of interalveolar septa from non-diabetic (NC) and untreated-diabetic (UD) rat lungs at different sacrifice periods. A: overview of alveolar wall of an NC rat sacrificed at 6 weeks showing type 1 alveolar epithelial cells (ep1) turned into the alveolar lumen (AL) and endothelial cells (en) of an alveolar capillary with erythrocytes (er) into the

capillary lumen. Note that alveolar and endothelial cells are separated by a thin fused basal laminae (bl); B: detail of an interalveolar septum of an NC rat sacrificed at 26 weeks with erythrocytes (er), endothelial capillary cells (en), type 1 alveolar epithelial cells (ep1), and a thin fused basal laminae (bl); C: type 2 alveolar epithelial cell of an NC rat sacrificed at 26 weeks with abundant microvilli (mi) protruding into the alveolar lumen (AL). Note the cytoplasm containing the characteristic osmiophilic lamellar bodies (lb), which store surfactant, and a rich complement of organelles such as endoplasmic reticulum (eR) and mitochondria (m); D: interalveolar septa of a UD rat sacrificed at 26 weeks with type 1 alveolar epithelial cells (ep1) disposed on the alveolar epithelial basal laminae (AEbl) with varying degrees of thickening. The capillary lumen (CL) is partially collapsed and surrounded by the endothelium (en) containing a large number of plasmalemmal vesicles (clear cells). Endothelial cells resting on the endothelial capillary basal laminae (ECbl), which is intensely thickened; E: portion of an alveolar septum of a UD rat sacrificed at 26 weeks showing thickening of endothelial capillary basal laminae (ECbl) and expansion of the interstitial extracellular matrix (em), which is characterized by the infiltration of edema, and abundant pynocytotic vesicles (v), collagen bands (co), elastin (el) and fibroblast-like cells (Fb); F: small portion of an alveolar septum of a UD rat sacrificed at 26 weeks showing numerous corpuscles of Weibel-Palade (W) and plasmalemmal vesicles (v); G: type 2 alveolar epithelial cell of a UD rat sacrificed at 26 weeks with few microvilli (mi) protruding into the alveolar lumen (AL). Note that the cell cytoplasm is poor in organelles and contains a higher amount of remnants of mature surfactant-rich lamellar bodies (lb) than in the NC rat; H-I: illustration of two fused basal laminae (bl) of alveolar septa from rats sacrificed at 26 weeks showing remarkable thickening in UD (H) compared with that observed in NC rat lung (I). Micrographs with 17,000 (A) and 42,000x final magnifications (B-I).

Ultrastructural morphometric analysis of the AE and EC basal laminae

The AE and EC basal laminae were significantly thicker in UD rat lungs than in NC rats (P<.01) throughout the study. There were no significant differences in the morphometric measurements of both basal laminae in lungs of UD rats sacrificed at 6, 14 or 26 weeks of follow-up. Table 5 shows the measurements of AE and EC basal laminae in rat lungs from the two experimental groups.

Table 5: Mean ± SD of thickness of the alveolar epithelial (AE) basal laminae and the endothelial capillary (EC) basal laminae in lungs of rats from the two experimental groups.

	Parameters		
Groups	**Follow-up (weeks)**	**AE basal laminae (µm)**	**EC basal laminae (µm)**
NC	6	0.0876 ± 0.0032	0.1612 ± 0.0115
	14	0.1034 ± 0.0038	0.1802 ± 0.0105
	26	0.0845 ± 0.0028	0.1492 ± 0.0112
UD	6	0.1543 ± 0.0028*	0.2440 ± 0.1240*
	14	0.1635 ± 0.0040*	0.2836 ± 0.0130*
	26	0.1803 ± 0.0020*	0.3004 ± 0.0138*

NC < UD: P<.01 at 6, 14 and 26 wks.

DISCUSSION

Despite the negative impact of diabetes mellitus (DM) on quality of life and survival of diabetic patients, the pathophysiological mechanisms involved in the genesis and progression of chronic diabetic lesions are still not fully known. Thus, the use of appropriate animal models that closely mimic the changes observed in humans is considered of utmost importance for filling these knowledge gaps.

This study showed that intravenous administration of alloxan is capable of inducing persistent diabetes in the rat, characterized by clinical signs of severe diabetes associated with a chronic state of hyperglycemia and hypoinsulinemia, with high levels of glycosylated hemoglobin. As previously observed in our laboratory while studying kidneys, eyes and rat nerves, [12.13.14], we observed that alloxan-induced diabetes was also capable of inducing characteristic histological and ultrastructural changes in the lungs, which may be considered a suitable model for studies of diabetic chronic lung disease.

However, diabetic lung lesions have been poorly explored in the literature, with few long-term studies describing the course of histopathological changes under a chronic hyperglycemia regime without any metabolic control. These alterations could explain the several abnormalities of the respiratory function observed in diabetic patients.[4.5]; however, the real implications of these changes in clinical practice are still very controversial.[15]

In this study, we found that fresh and fixed lung weights were significantly reduced in untreated diabetic (UD) rats compared with those in non-diabetic control (NC) rats, although they were increased in relation to body weight. Fixed lung volume and lung compliance were also significantly decreased in diabetic rats throughout the study. These findings have also been reported by

others. Ofulue et al. [16] found that specific lung volume and weight in relation to body weight were increased in streptozotocin (STZ)-induced diabetic rats at 7 weeks of diabetes. Sahebjami & Denholm.[17] observed that dry weight, air and saline lung volumes, and lung compliance were significantly lower in both young and adult STZ-induced diabetic rats compared with controls at 8 weeks of diabetes.

Reduction in the lung mass and volume, with retraction and compliance loss in diabetes, may be a result of increased amounts of collagen and elastin related to the biochemical alteration of connective tissue components induced by chronic hyperglycemia. Ofulue et al. [16.18] confirmed this hypothesis when they found that the amounts of collagen and elastin were increased in lungs of STZ-induced diabetic rats, whereas degradation of connective tissue was decreased. These alterations could explain in part the reduced pulmonary elastic recoil and the restrictive ventilatory changes observed in diabetic patients.[19.20]

According to Sandler.[21] it is possible that the prolonged exposure of connective tissue proteins to hyperglycemia may result in excessive nonenzymatic glycosylation (NEG) of lysine or hydroxylysine residues and the development of impaired or abnormal cross-links. Because cross-linking of collagen and elastin is important in conferring both strength and elasticity to lung connective tissue, excessive NEG may result in impairment of lung properties. This hypothesis has been postulated previously by others.[22]

We also found that UD rats showed innumerous morphological changes in the lungs that affected almost the entire pulmonary parenchyma. These changes were progressive and were closely correlated with diabetes duration. Diabetic microangiopathy in the lung was found to involve the capillaries of alveolar septa and was manifested by congestion, insudation, intra-alveolar plasmorrhagy, interstitial inflammatory infiltrate, thickening of the basal laminae, and expansion of interstitial extracellular matrix. These findings were also observed by Kodolova et al.[7] while studying the lungs of autopsied patients with DM at various degrees of severity and duration. Forgiarini-Jr et al.[23] also found an increase in the extracellular matrix in STZ-induced diabetic rats, as evidenced by the presence of an inflammatory process in lung tissue as well as an increase in the thickness of the alveolar-capillary membrane and fibrosis.

Alveolar perimeter and alveolar surface area were also significantly reduced in UD rats in our study. Consequently, the total number of alveoli in the lungs of these rats was higher than that observed in the controls. More alveoli per unit volume with a decrease in the surface area and an increase in the surface-to-volume ratio were also observed by Kida et al.[24] in lungs of growing STZ diabetic rats. Similar findings were also reported by others.[16]

Despite all of the morphological and morphometric changes observed in pulmonary tissue of alloxan-induced diabetic rats, we found no lesions or fatty deposits in the endothelium of the pulmonary arteries and their trunks. This finding has already been previously observed in our laboratory studying the aorta and the iliac, renal and coronary arteries of diabetic Wistar rats, even in those sacrificed at 50 weeks after diabetes induction.[25] Despite abnormalities observed in the lipid metabolism of the pulmonary artery and lungs during insulin deficiency, Reinilä et al. also found no injuries in elastic arteries (aorta, main pulmonary arteries) of STZ diabetic rats two months after diabetes induction.[26] However, these authors found significant basement membrane thickening of smooth muscle cells of the muscular pulmonary arteries in 40% of diabetic animals. From our perspective, the rat may not be a suitable model of diabetic macroangiopathy because of having elevated heart rate (350-450 bpm) and slightly lower systolic blood pressure than that observed in humans.[27]

In this study, we also found ultrastructural changes compromising the alveolar septa that included the thickening of alveolar epithelial (AE) and endothelial capillary (EC) basal laminae, the narrowing of the alveolar and capillary lumen, the degeneration and atrophy of type I alveolar epithelial cells, the expansion of interstitial extracellular matrix by edema and abundant pynocytotic vesicles, and evident ultrastructural disorganization of type II alveolar epithelial cells. These ultrastructural changes were progressively and closely correlated with diabetes duration and were markedly severe in diabetic rats sacrificed at 26 weeks of diabetes.

The thickening of AE and EC basal laminae is considered an ultrastructural hallmark in diabetic patients and in animal models of diabetes. [28] Vracko et al. [29], while studying lungs from autopsied patients, found that these basement membranes were significantly thicker in diabetic patients than they were in age-matched control subjects. Similar results were also found by Weynand et al. [30] in lung and kidney autopsied samples from 6 diabetics and 6 control subjects. However, in contrast to our findings, the degree of thickening of both membranes as observed by the two mentioned studies did not correlate significantly with patient age or with known duration of diabetes. Those authors admitted, however, that failures in the analysis of this correlation may have occurred because the actual diabetes duration was not well known in many patients.

A narrowed or collapsed alveolar and capillary lumen associated with EC basal laminae thickening was also found by Popov & Simionescu [8.31] while studying mice and hamsters rendered diabetic by STZ at time intervals ranging from 2-24 weeks after diabetes induction. Similar to our findings, these authors also observed

hyperplasia of the extracellular matrix, which was rich in collagen bundles, with numerous plasmalemmal vesicles in the capillary endothelium and Weibel-Palade bodies in the venular endothelium. These signs are indicative of severe inflammatory and thrombogenic responses of the vascular endothelium, as well as high transcytosis of macromolecules through the cell membranes.

Alterations of type II alveolar epithelial cells were also observed by Sugahara et al.[6] in approximately 50% of alloxan-induced diabetic rats sacrificed at 2 weeks of diabetes and 87.5% at 4 weeks. In this latter sacrifice period, the average number of lamellar inclusion bodies decreased to approximately half of that of the control animals. This finding was also reported by others [23.32], suggesting that surfactant production was reduced in UD rats. In our study, however, the number of lamellar bodies was apparently normal, but type II alveolar epithelial cells had a significant diminution in the number of microvilli and a high amount of mature lamellar corpuscles, with a delay in their surfactant output out of the cytoplasm. Despite the decreased amount of lamellated bodies, all other findings observed in the type II alveolar epithelial cells from rat lungs in our study were confirmed by Lysenko et al.[32]

Macroscopy, morphological, morphometric, and ultrastructural changes observed in rat lungs support the conclusion that the lungs, such as the kidneys, eyes and nerves, may also be considered a target organ of diabetes and may explain the various functional respiratory disturbances observed in diabetic subjects. Nonetheless, the pathophysiological mechanisms involved in the genesis and progression of chronic diabetic lesions of the lungs and other organs are not yet fully known. Evidence that elevated reactive oxygen species (ROS) generation and altered redox balance may be present during the glucose auto-oxidation process and protein glycation has suggested that oxidative damage plays a key role in the genesis of diabetic complications.[33.34]

The results of the present study strongly suggest that oxidative stress is also seen in pulmonary tissue from alloxan-induced diabetic rats, as demonstrated by elevated LPO concentrations and reduced SOD, CAT, and GSH-Px activities. In this study, pulmonary oxidative stress also had a strong relationship with diabetes duration; this association was more intense after 14 weeks of diabetes. Similar results were also reported by others.[35.36.37]

Nevertheless, it is controversial whether oxidative damage induces or promotes diabetic lesions, or whether it is simply just one step in a complex phenomenon with several other mechanisms.[38] However, it is widely known that oxidative damage can play an important role in regulating cellular adhesion, proliferation, migration, and cell signaling of the extracellular matrix [39] and may alter the structure and permeability of the cellular membrane and intracellular organelles such as mitochondria and rough endoplasmic reticulum. These factors affect ionic turnover through the membrane, cellular oxidative process, and protein synthesis. [40] ROS generation may also attack lysosomes and cellular DNA, making the cell more susceptible to damage from toxic products and mutations that can lead to cell death.[40.41]

Oxidative stress does not seem to be a solitary pathway in the development of diabetic complications as demonstrated in several studies, involving mainly kidney lesions. [38.39.42.43.44] One well-known mechanism of cellular damage is mediated by advanced glycation end-products (AGE). These substances result from protein peroxidation and may inactivate various enzymes responsible for molecular turnover at cellular membranes and organelles.[42.43.45] In the lungs, abnormalities observed in connective tissue synthesis and turnover may be secondary to the NEG process and AGE.[42.43] and may lead to thickening of the basement membranes in capillaries, as shown in our and other studies either in the AE or EC basal laminae.[7.29.30]

Another harmful mechanism observed in glucose-independent tissues (e.g., nervous tissue) is activation of polyol enzyme pathways, where hyperglycemia may increase sorbitol levels in the cells, elevating their osmolarity, which may cause cellular death.[38] Hyperglycemia may also activate the hexosamine pathway, which is responsible for converting glucose into compounds derived from acetylglucosamine that modulate the expression of various proteins and substances, such as plasminogen activator inhibitor-1 (PAI-1) and transforming growth factor-beta 2 (TGFβ2), which may contribute to the vascular thrombosis and excessive production of collagen matrix on the vascular endothelium. These mechanisms are directly implicated in the genesis and evolution of diabetic microangiopathy.[39] Augmented production of protein kinase-C (PKC) formed from free fatty acid oxidation may reduce nitric oxide concentrations in diabetic tissue and also elevate the amount of TGFβ2 and vascular endothelial growth factor-A (VEGF-A). These substances may primarily contribute to narrowing of the capillary net, a reduction in vascular blood flow, and an increase in collagen matrix deposits on the vascular endothelium, elevating the risks of vascular thrombosis and occlusions.[44]

CONCLUSIONS

Alloxan-diabetes causes morphological, morphometric and ultrastructural changes in rat lungs, demonstrating that these organs may also be considered a target of diabetes. It may also explain the various functional respiratory disturbances observed in diabetic subjects. The observed changes may be strongly correlated with oxidative imbalance caused by persistent hyperglycemia, indicating that any treatment proposed to prevent, stabilize, or reverse chronic diabetic lesions must first include the effective control of hyperglycemia, which seems to be the only way to control ROS and AGE

generation as well as the mechanisms directly involved in the molecular pathways responsible for cellular damage in diabetes.

ACKNOWLEDGEMENTS

We thank to Professors Júlio Defavari and Deilson Elgui de Oliveira from the Department of Pathology, Faculty of Medicine Botucatu – UNESP for assistance in the histopathological and morphometric analysis, and Professor Daniela Carvalho dos Santos from the Department of Morphology, Institute of Biosciences Botucatu – UNESP for assistance in the electron microscopy analysis.

REFERENCES

1. Nathan DM. Diabetes: advances in diagnosis and treatment. JAMA, 2015; 313(10): 1052-62.
2. Leon BM, Maddox TM. Diabetes and cardiovascular disease: Epidemiology, biological mechanisms, treatment recommendations and future research. World J Diabetes, 2015; 6(13): 1246-58.
3. Ahlqvist E, van Zuydam NR, Groop LCm McCarthy MI. The genetic of diabetic complications. Nat Rev Nephrol, 2015; 11(5): 277-87.
4. Sandler M, Bumm AE, Stemont RI. Cross-section study of pulmonary function in patients with insulin-dependent diabetes mellitus. Am Rev Respir Dis, 1987; 135(5): 223-9.
5. Innocenti F, Fabbri A, Anichini R, Tuci S, Pettinà G, Vannucci F, De Giorgio LA, Seghieri G. Indications of reduced pulmonary function in type 1 (insulin-dependent) diabetes mellitus. Diabetes Res Clin Pract, 1994; 25(3): 161-8.
6. Sugahara K, Ushijima K, Morioka T, Usuku G. Studies of the lung in diabetes mellitus. I - Ultrastructural studies of the lungs in alloxan-induced diabetic rats. Virchows Arch A Pathol Anat Histol, 1981; 390(3): 313-24.
7. Kodolova IM, Lysenko LV, Saltykov BB. Changes in the lungs in diabetes mellitus. Arkh Patol, 1982; 44(7): 35-40.
8. Popov D, Simionescu M. Alterations of lung structure in experimental diabetes and diabetes associated with hyperlipidaemia in hamsters. Eur Resp J, 1997; 10(8): 1850-8.
9. Nerup J, Mandrup-Poulsen T, Helqvist S, Andersen HU, Pociot F, Reimers JI, Cuartero BG, Karlsen AE, Bjerre U, Lorenzen T. On the pathogenesis of IDDM. Diabetologia, 1994; 37(suppl 2): S82-9.
10. Allen DA, Yaqoob MM, Harwood SM. Mechanisms of high glucose-induced apoptosis and its relationship to diabetic complications. J Nutr Biochem, 2005; 16(12): 705-13.
11. Spadella CT, Machado JLM, Lerco MM, Ortolan EV, Marques SF. Pancreas transplantation prevents cellular oxidative stress in kidneys of alloxan-induced diabetic rats. Transpl Proc, 2008; 40(2); 524-8.
12. Spadella CT, Lerco MM, Machado JL, Macedo CS. Long-term effects of insulin therapy, islet transplantation, and pancreas transplantation in the prevention of glomerular changes in kidneys of alloxan-induced diabetic rats. Transplant Proc, 2005; 37(8): 3468-71.
13. Spadella CT, Machado JL, Lerco MM, Ortolan EV, Schellini SA, Gregório EA. Temporal relationship between successful pancreas transplantation and control of ocular complications in alloxan-induced diabetic rats.Transplant Proc, 2008; 40(2): 518-23.
14. Spadella CT, Machado JL, Caramori CA, Gregório EA. Successful islet transplantation does not prevent the development of neuropathy in alloxan-induced diabetic rats. Transplant Proc, 2002; 34(4): 1296-300.
15. Pitocco D, Fuso L, Conte EG, Zaccardi F, Condoluci C, Scavone G, Incalzi RA, Ghirlanda G. The diabetic lung – a new target organ? Rev Diabet Stud, 2012; 9(1): 23-35.
16. Ofulue AF, Kida K, Thurlbeck WM. Experimental diabetes and the lung. I. Changes in growth, morphometry, and biochemistry. Am Rev Respir Dis, 1988; 137(1): 162-6.
17. Sahebjiami H, Denholm D. Effects of streptozotocin-induced diabetes on lung mechanics and biochemistry in rats. J Appl Physiol, 1985; 64(1): 147-53.
18. Ofulue AF, Thurlbeck M. Experimental diabetes and the lung. II. In vivo connective tissue metabolism. Am Rev Respir Dis, 1988; 138(2): 284-9.
19. Shah SH, Sonawane P, Nahar P, Vaidya S, Salvi S. Pulmonary function tests in type 2 diabetes mellitus and their association with glycemic control and duration of the disease. Lung India, 2013; 30(2): 108-12.
20. Marvisi M, Marani G, Brianti M, Della Porta R. Pulmonary complications in diabetes mellitus. Recenti Prog Med, 1996; 87(12): 623-7.
21. Sandler M. Is the lung a “target organ” in diabetes mellitus? Arch Intern Med, 1990; 150(7): 1385-8.
22. Madia Am, Rozovski SJ, Kagan HM. Changes in lung lysyl oxidase activity in streptozotocin-diabetes and in starvation. Biochem Biophys, 1979; 585(4): 481-7.
23. Forgiarini-Jr LA, Kretzmann NA, Tieppo J, Picada JN, Dias AS, Marroni NAP. Lung alterations in a rat model of diabetes mellitus: effects of antioxidant therapy. J Bras Pneumol, 2010; 36(5): 579-87.
24. Kida K, Utsuyama M, Takizawa T, Thurlbeck WM. Changes in lung morphological features in elasticity caused by streptozotocin-induced diabetes mellitus in growing rats. Am Rev Respir Dis, 1983; 128(1): 125-31.
25. Lerco MM. (2000). Characterization of an experimental model of diabetes mellitus induced by alloxan. Clinical, laboratory, and histopathological studies of the kidney, retina, coronary, aorta, and iliac artery of rats. [Masters Dissertation]. Sao Paulo State University, UNESP, Brazil.

26. Reinilä A. Long-term effects of untreated diabetes on the arterial wall in rat. An ultrastructural study. Diabetologia, 1981; 20(3): 205-12.
27. Büttner D, Hackbarth H, Wollnik F, Borggreve H. Blood pressure in rats: a comparison of a multifactorial experimental design to measurements in an outbred stock. Lab Animals, 1984; 18(2): 110-4.
28. Carlson EC, Audette JL, Veitenheimer NJ, Risan JA, Laturnus DI, Epstein PN. Ultrastructural morphometry of capillary basement membrane thickness in normal and transgenic diabetic mice. Anat Rec A Discov Mol Cell Evol Biol, 2003; 271(2): 332-41.
29. Vracko R, Thorning D, Huang TW. Basal lamina of alveolar epithelium and capillaries: quantitative changes with aging and in diabetes mellitus. Am Rev Respir Dis, 1979; 120(5): 973-83.
30. Weynand B, Jonckheere A, Frans A, Rahier J. Diabetes mellitus induces a thickening of the pulmonary basal lamina. Respiration, 1999; 66(1): 14-9.
31. Popov D, Simionescu M. Structural and transport property alterations of the lung capillary endothelium in diabetes. Ital J Anat Embryol, 2001; 106(2 suppl 1): 405-12.
32. Lysenko LV, Lysenko AL, Kulik VP. Ultrastructural and ultracytochemical changes in the lungs of rats with diabetes mellitus. Biull Eksp Biol Med, 1990; 109(1): 75-8.
33. Rahimi R, Nikfar S, Larijani B. A review on the role of antioxidants in the management of diabetes and its complication. Biomed Pharmacother, 2005; 59(7): 365-73.
34. Rolo AP, Palmeira CM. Diabetes and mitochondrial function: role of hyperglycemia and oxidative stress. Toxicol Appl Pharmacol, 2006; 212(2): 167-78.
35. Gumieniczek A, Hopkala H, Wójtowicz Z, Wysocka M. Changes in antioxidant status of lung tissue in experimental diabetes in rabbits. Clin Biochem, 2002; 35(2): 147-9.
36. Hürdag C, Uyaner L, Gürel E, Utkusavas A, Atukeren P, Demirci C. Effect of apha-lipoic acid on NOS dispersion in the lung of streptozotocin-induced diabetic rats. J Diabet Compl, 2008; 22(1): 56-61.
37. Sacan O, Turkyilmaz IB, Bayrak BB, Mutlu O, Akev N, Yanardag R. Zinc supplementation ameriolates glycoprotein componentes and oxidative stress changes in the lung of streptozotocin diabetic rats. Biometals, 2016; 29(2): 239-48.
38. Khan ZA, Farhangkhoee H, Chakrabarti S. Towards newer molecular targets for chronic diabetic complications. Curr Vasc Pharmacol, 2006; 4(1): 45-57.
39. Rees MD, Kennett EC, Whitelock JM, Davies MJ. Oxidative damage to extracellular matrix and its role in human pathologies. Free Radic Med, 2008; 44(12): 1973-2001.
40. Blokhina O, Virolainen E, Fagerstedt KV. Antioxidants, oxidative damage and oxygen deprivation stress: a review. Ann Bot, 2003; 91(2): 179-94.
41. Niedowicz DM, Daleke Dl. The role of oxidative stress in diabetic complications. Cell Biochem Biophys, 2005; 43(2): 289-330.
42. Tan AL, Forbes JM, Cooper ME. AGE, RAGE, and ROS in diabetic nephropathy. Semin Nephrol, 2007; 27(2): 130-43.
43. Thomas MC, Forbes JM, Cooper ME. Advanced glycation end products and diabetic nephropathy. Am J Ther, 2005; 12(6): 562-72.
44. Ohshiro Y, Takasu N. Molecular mechanisms of diabetic nephropathy. Nippon Rinsho, 2006; 64(5): 997-1003.
45. Vincent AM, Russell JW, Low P, Feldman EL. Oxidative stress in pathogenesis of diabetic neuropathy. Endocr Rev, 2004; 25(4): 612-28.